Chapter 7

Dispersion, Impedance, Reflection, and Transmission

7.1 Introduction

A dispersion relation gives the relationship between frequency and the speed of propagation. This relationship is rather simple in the continuous world and is reviewed in the next section. Unfortunately dispersion in the FDTD is not as simple. Nevertheless, it provides a great deal of insight into the inherent limitations of the FDTD method and hence it is important that one have at least a basic understanding of it.

The tools developed in the analysis of FDTD dispersion can also be used to determine the characteristic impedance of the grid. Furthermore, as will be shown, knowing the dispersion relationship one can obtain exact analytic expressions for the reflection and transmission coefficients in the FDTD grid.

7.2 Dispersion in the Continuous World

Consider a plane wave propagating in the $+x$ direction in a lossless medium. In time-harmonic form the temporal and spatial dependence of the wave are given by $\exp(j[\omega t - \beta x])$ where ω is the frequency and β is the phase constant (wave number). The speed of the wave can be found by determining how fast a given point on the wave travels. In this context "point" is taken to mean a point of constant phase. The phase is dictated by $\omega t - \beta x$. Setting this equal to a constant and differentiating with respect to time gives

$$\frac{d}{dt}(\omega t - \beta x) = \frac{d}{dt}(\text{constant}), \tag{7.1}$$

$$\omega - \beta \frac{dx}{dt} = 0. \tag{7.2}$$

In this expression x is taken to be the position which provides a particular phase. In that sense it is not an independent variable. The location x which yields the desired phase will change as a

[†]Lecture notes by John Schneider. `fdtd-dispersion.tex`

function of time. Therefore, dx/dt is the speed of the wave, or, more properly, the phase speed c_p. Solving (7.2) for the phase speed yields

$$c_p = \frac{dx}{dt} = \frac{\omega}{\beta}. \tag{7.3}$$

This is apparently a function of frequency, but for a plane wave the phase constant β is given by $\omega\sqrt{\mu\epsilon}$. Thus the phase speed is

$$c_p = \frac{\omega}{\omega\sqrt{\mu\epsilon}} = \frac{1}{\sqrt{\mu_r\mu_0\epsilon_r\epsilon_0}} = \frac{c}{\sqrt{\mu_r\epsilon_r}} \tag{7.4}$$

where c is the speed of light in free space. Note that, in the continuous world for a lossless medium, the phase speed is independent of frequency and the dispersion relationship is

$$c_p = \frac{\omega}{\beta} = \frac{c}{\sqrt{\mu_r\epsilon_r}}. \tag{7.5}$$

Since c is a constant, and we are assuming μ_r and ϵ_r contact for the given material, all frequencies propagate at the same speed. Unfortunately this is not the case in the discretized FDTD world—different frequencies have different phase speeds.*

7.3 Harmonic Representation of the FDTD Method

The spatial shift-operator s_x and the temporal shift-operator s_t were introduced in Sec. 6.5. Generalizing these slightly, let a fractional superscript represent a corresponding fractional step. For example,

$$s_x^{1/2} H_y^q[m] = H_y^q\left[m + \frac{1}{2}\right], \tag{7.6}$$

$$s_t^{1/2} E_z^{q+\frac{1}{2}}[m] = E_z^{q+1}[m], \tag{7.7}$$

$$s_t^{-1/2} E_z^{q+\frac{1}{2}}[m] = E_z^q[m]. \tag{7.8}$$

Using these shift operators the finite-difference version of Ampere's law (ref. (3.17)) can be written

$$\epsilon\left(\frac{s_t^{1/2} - s_t^{-1/2}}{\Delta_t}\right) E_z^{q+\frac{1}{2}}[m] = \left(\frac{s_x^{1/2} - s_x^{-1/2}}{\Delta_x}\right) H_y^{q+\frac{1}{2}}[m]. \tag{7.9}$$

Note that both fields have a temporal index of $q + 1/2$. The index can be changed to q if the $1/2$ is accounted for by a temporal shift. Thus Ampere's law can also be written

$$s_t^{1/2}\epsilon\left(\frac{s_t^{1/2} - s_t^{-1/2}}{\Delta_t}\right) E_z^q[m] = s_t^{1/2}\left(\frac{s_x^{1/2} - s_x^{-1/2}}{\Delta_x}\right) H_y^q[m]. \tag{7.10}$$

*Later we will consider FDTD models of materials that are dispersive in the continuous world, i.e., materials for which ϵ or μ are functions of frequency. In fact, we have already considered dispersive behavior to some degree since lossy materials have phase speeds that are a function of frequency.

Let us define the finite-difference operator $\tilde{\partial}_i$ as

$$\tilde{\partial}_i = \left(\frac{s_i^{1/2} - s_i^{-1/2}}{\Delta_i} \right) \tag{7.11}$$

where i is either x or t. Using this notation the Yee version of Ampere's law can be written

$$\epsilon s_t^{1/2} \tilde{\partial}_t E_z^q[m] = s_t^{1/2} \tilde{\partial}_x H_y^q[m] \,. \tag{7.12}$$

Rather than obtaining an update equation from this, the goal is to determine the phase speed for a given frequency. To that end, we assume there is a single harmonic wave propagating such that

$$\hat{E}_z^q[m] = \hat{E}_0 e^{j(\omega q \Delta_t - \tilde{\beta} m \Delta_x)}, \tag{7.13}$$

$$\hat{H}_y^q[m] = \hat{H}_0 e^{j(\omega q \Delta_t - \tilde{\beta} m \Delta_x)}, \tag{7.14}$$

where $\tilde{\beta}$ is the phase constant which exists in the FDTD grid and $\hat{E}_0$ and $\hat{H}_0$ are constant amplitudes. A tilde will be used to indicate quantities in the FDTD grid which will typically (but not always!) differ from the corresponding value in the continuous world. Thus, the phase constant $\tilde{\beta}$ in the FDTD grid will differ, in general, from the phase constant β in the continuous world. As was done in Sec. 5.8 a caret (hat) will be used to indicate a harmonic quantity.

We will assume the frequency ω is the same in both the FDTD grid and the continuous world. Note that one has complete control over the frequency of the excitation—one merely has to ensure that the phase of the source changes a particular number of radians every time step. However, one does not have control over the phase constant, i.e., the spatial frequency. The grid dictates what $\tilde{\beta}$ will be for a given temporal frequency.

The plane-wave space-time dependence which appears in (7.13) and (7.14) essentially serves as an eigenfunction for the FDTD governing equations. If the governing equations operate on a function with this dependence, they will yield another function which has the same space-time dependence, albeit scaled by some value. To illustrate this, consider the temporal shift-operator acting on the electric field

$$\begin{aligned} s_t^{\pm 1/2} \hat{E}_z^q[m] &= \hat{E}_0 e^{j[\omega(q \pm 1/2)\Delta_t - \tilde{\beta} m \Delta_x]} \\ &= e^{\pm j\omega\Delta_t/2} \hat{E}_0 e^{j[\omega q \Delta_t - \tilde{\beta} m \Delta_x]} \\ &= e^{\pm j\omega\Delta_t/2} \hat{E}_z^q[m] \,. \end{aligned} \tag{7.15}$$

Similarly, the spatial shift-operator acting on the electric field yields

$$\begin{aligned} s_x^{\pm 1/2} \hat{E}_z^q[m] &= \hat{E}_0 e^{j[\omega q \Delta_t - \tilde{\beta}(m \pm 1/2)\Delta_x]} \\ &= e^{\mp j\tilde{\beta}\Delta_x/2} \hat{E}_0 e^{j[\omega q \Delta_t - \tilde{\beta} m \Delta_x]} \\ &= e^{\mp j\tilde{\beta}\Delta_x/2} \hat{E}_z^q[m] \,. \end{aligned} \tag{7.16}$$

Thus, for a plane wave, one can equate the shift operators with multiplication by an appropriate term:

$$s_t^{\pm 1/2} \Leftrightarrow e^{\pm j\omega\Delta_t/2}, \tag{7.17}$$

$$s_x^{\pm 1/2} \Leftrightarrow e^{\mp j\tilde{\beta}\Delta_x/2}. \tag{7.18}$$

Carrying this a step further, for plane-wave propagation the finite-difference operators $\tilde{\partial}_t$ and $\tilde{\partial}_x$ are equivalent to

$$\tilde{\partial}_t = \frac{e^{+j\omega\Delta_t/2} - e^{-j\omega\Delta_t/2}}{\Delta_t} = j\frac{2}{\Delta_t}\sin\left(\frac{\omega\Delta_t}{2}\right), \tag{7.19}$$

$$\tilde{\partial}_x = \frac{e^{-j\tilde{\beta}\Delta_x/2} - e^{+j\tilde{\beta}\Delta_x/2}}{\Delta_x} = -j\frac{2}{\Delta_x}\sin\left(\frac{\tilde{\beta}\Delta_x}{2}\right). \tag{7.20}$$

We define Ω and K_x as

$$\Omega = \frac{2}{\Delta_t}\sin\left(\frac{\omega\Delta_t}{2}\right), \tag{7.21}$$

$$K_x = \frac{2}{\Delta_x}\sin\left(\frac{\tilde{\beta}\Delta_x}{2}\right). \tag{7.22}$$

Note that as the discretization goes to zero, Ω approaches ω and K_x approaches $\tilde{\beta}$ (and, in fact, $\tilde{\beta}$ would approach β, the phase constant in the continuous world). Using this notation, taking a finite-difference with respect to time is equivalent to multiplication by $j\Omega$ while a finite difference with respect to space is equivalent to multiplication by $-jK_x$, i.e.,

$$\tilde{\partial}_t \Leftrightarrow j\Omega \tag{7.23}$$

$$\tilde{\partial}_x \Leftrightarrow -jK_x. \tag{7.24}$$

Using (7.17), (7.23), and (7.24) in Ampere's law (7.12) yields

$$j\epsilon\Omega e^{j\omega\Delta_t/2}\hat{E}_z^q[m] = -jK_x e^{j\omega\Delta_t/2}\hat{H}_y^q[m]\,. \tag{7.25}$$

The temporal shift $\exp(j\omega\Delta_t/2)$ is common to both side and hence can be canceled. Using the assumed form of the electric and magnetic fields from (7.13) and (7.14) in (7.25) yields

$$\epsilon\Omega\hat{E}_0 e^{j(\omega q\Delta_t - \tilde{\beta}m\Delta_x)} = -K_x\hat{H}_0 e^{j(\omega q\Delta_t - \tilde{\beta}m\Delta_x)}. \tag{7.26}$$

Canceling the exponential space-time dependence which is common to both sides produces

$$\epsilon\Omega\hat{E}_0 = -K_x\hat{H}_0. \tag{7.27}$$

Solving for the ratio of the electric and magnetic field amplitudes yields

$$\frac{\hat{E}_0}{\hat{H}_0} = -\frac{K_x}{\epsilon\Omega} = -\frac{\Delta_t}{\epsilon\Delta_x}\frac{\sin\left(\frac{\tilde{\beta}\Delta_x}{2}\right)}{\sin\left(\frac{\omega\Delta_t}{2}\right)}. \tag{7.28}$$

It appears that (7.28) is the "numeric impedance" since it is the ratio of the electric field to the magnetic field. In fact it *is* the numeric impedance, but it is only part of the story. As will be shown, the impedance in the FDTD method is exact. This fact is far from obvious if one only considers (7.28). It is also worth considering the corresponding continuous-world quantity $\beta/(\epsilon\omega)$:

$$\frac{\beta}{\epsilon\omega} = \frac{\omega/c_p}{\epsilon\omega} = \frac{1}{\epsilon c_p} = \frac{\sqrt{\mu\epsilon}}{\epsilon} = \sqrt{\frac{\mu}{\epsilon}} = \eta \tag{7.29}$$

Thus the fact that the grid numeric impedance is given by $K_x/(\epsilon\Omega)$ is consistent with continuous-world behavior. (The negative sign in (7.28) merely accounts for the orientation of the fields.)

7.4 Dispersion in the FDTD Grid

Another equation relating $\hat{E}_0$ and $\hat{H}_0$ can be obtained from Faraday's law. Expressed in terms of shift operators, the finite-difference form of Faraday's law (ref. (3.14)) is

$$\mu s_x^{1/2}\tilde{\partial}_t \hat{H}_y^q[m] = s_x^{1/2}\tilde{\partial}_x \hat{E}_z^q[m]\,. \tag{7.30}$$

As before, assuming plane-wave propagation, the shift operators can be replaced with multiplicative equivalents. The resulting equation is

$$j\mu\Omega e^{-j\omega\Delta_x/2}\hat{H}_y^q[m] = -jK_x e^{-j\omega\Delta_x/2}\hat{E}_z^q[m]\,. \tag{7.31}$$

Canceling terms common to both sides and rearranging yields

$$\frac{\hat{E}_0}{\hat{H}_0} = -\frac{\mu\Omega}{K_x} = -\frac{\mu\Delta_x}{\Delta_t}\frac{\sin\left(\frac{\omega\Delta_t}{2}\right)}{\sin\left(\frac{\tilde{\beta}\Delta_x}{2}\right)}. \tag{7.32}$$

Equating (7.28) and (7.32) and cross-multiplying gives

$$\mu\epsilon\Omega^2 = K_x^2. \tag{7.33}$$

This is the FDTD dispersion relation. Alternatively, expanding terms and rearranging slightly yields

$$\sin^2\left(\frac{\omega\Delta_t}{2}\right) = \frac{\Delta_t^2}{\epsilon\mu\Delta_x^2}\sin^2\left(\frac{\tilde{\beta}\Delta_x}{2}\right). \tag{7.34}$$

Taking the square root of both sides of either form of the dispersion relation yields

$$\sqrt{\mu\epsilon}\Omega = K_x, \tag{7.35}$$

or

$$\sin\left(\frac{\omega\Delta_t}{2}\right) = \frac{\Delta_t}{\sqrt{\epsilon\mu}\Delta_x}\sin\left(\frac{\tilde{\beta}\Delta_x}{2}\right). \tag{7.36}$$

These equations dictate the relationship between ω and $\tilde{\beta}$. Contrast this to the dispersion relation (7.5) which pertains to the continuous world. The two appear quite dissimilar! However, the two equations do agree in the limit as the discretization gets small.

The first term in the Taylor series expansion of $\sin(\xi)$ is ξ. Thus ξ provides a good approximation of $\sin(\xi)$ when ξ is small. Assume that the spatial and temporal steps are small enough so that the arguments of the sine functions in (7.36) are small. Retaining the first-order term in the Taylor-series expansion of the sine functions in (7.36) yields

$$\frac{\omega\Delta_t}{2} = \frac{\Delta_t}{\sqrt{\epsilon\mu}\Delta_x}\frac{\tilde{\beta}\Delta_x}{2}. \tag{7.37}$$

From this $\tilde{\beta}$ is seen to be

$$\tilde{\beta} = \omega\sqrt{\mu\epsilon}, \tag{7.38}$$

which is exactly the same as in the continuous world. However, this is only true when the discretization goes to zero. For finite discretization, the phase speed in the FDTD grid and in the continuous world differ.

In the continuous world the phase speed is $c_p = \omega/\beta$. In the FDTD world the same relation holds, i.e., $\tilde{c}_p = \omega/\tilde{\beta}$ where the tilde indicates this is the phase speed in the discretized world. In one dimension, a closed form solution for $\tilde{\beta}$ is possible (a similar dispersion relation holds in two and three dimensions, but there a closed-form solution is not possible). Bringing the coefficient to the other side of (7.36) and taking the arc sine yields

$$\frac{\tilde{\beta}\Delta_x}{2} = \sin^{-1}\left[\frac{\Delta_x\sqrt{\mu\epsilon}}{\Delta_t}\sin\left(\frac{\omega\Delta_t}{2}\right)\right]. \tag{7.39}$$

As was shown in Sec. 5.2.2 (ref. (5.7) and (5.8)), the factor $\omega\Delta_t/2$ is equivalent to $\pi S_c/N_\lambda$ where $S_c = c\Delta_t/\Delta_x$. Thus (7.39) can be written

$$\frac{\tilde{\beta}\Delta_x}{2} = \sin^{-1}\left[\frac{\sqrt{\mu_r\epsilon_r}}{S_c}\sin\left(\frac{\pi S_c}{N_\lambda}\right)\right]. \tag{7.40}$$

Consider the ratio of the phase speed in the grid to the true phase speed

$$\frac{\tilde{c}_p}{c_p} = \frac{\omega/\tilde{\beta}}{\omega/\beta} = \frac{\beta}{\tilde{\beta}} = \frac{\frac{\beta\Delta_x}{2}}{\frac{\tilde{\beta}\Delta_x}{2}}. \tag{7.41}$$

The phase constant in the continuous world can be written

$$\beta = \omega\sqrt{\mu\epsilon} = 2\pi\frac{c}{\lambda}\sqrt{\mu_0\epsilon_0\mu_r\epsilon_r} = \frac{2\pi}{\lambda}\sqrt{\mu_r\epsilon_r} = \frac{2\pi}{N_\lambda\Delta_x}\sqrt{\mu_r\epsilon_r} \tag{7.42}$$

where N_λ is the number of points per free-space wavelength. Using this in the numerator of the last term on the right-hand side of (7.41) and using (7.40) in the denominator, this ratio becomes

$$\frac{\tilde{c}_p}{c_p} = \frac{\pi\sqrt{\mu_r\epsilon_r}}{N_\lambda\sin^{-1}\left[\frac{\sqrt{\mu_r\epsilon_r}}{S_c}\sin\left(\frac{\pi S_c}{N_\lambda}\right)\right]}. \tag{7.43}$$

This equation is a function of the material parameters (ϵ_r and μ_r), the Courant number (S_c), and the number of points per wavelength (N_λ).

For propagation in free space, i.e., $\epsilon_r = \mu_r = 1$, when there are 20 points per wavelength and the Courant number S_c is $1/2$, the ratio of the numeric to the exact phase speed is approximately 0.9969 representing an error of 0.31 percent. Thus, for every wavelength of travel, the FDTD wave will accumulate about 1.12 degrees of phase error (0.0031×360). If the discretization is lowered to 10 points per wavelength, the ratio drops to 0.9873, or about a 1.27 percent error. Note that as the discretization was halved, the error increased by roughly a factor of four. This is as should be expected for a second-order method.

Consider the case of propagation in free space and a Courant number of 1. In that case the ratio collapses to

$$\frac{\tilde{c}_p}{c_p} = \frac{\pi}{N_\lambda\sin^{-1}\left[\sin\left(\frac{\pi}{N_\lambda}\right)\right]} = 1. \tag{7.44}$$

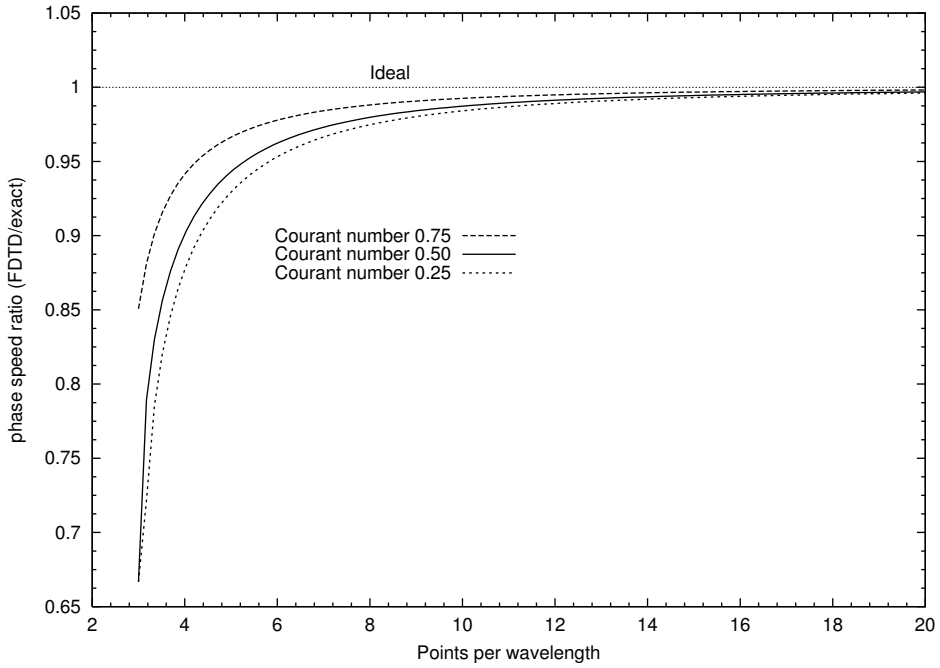

Figure 7.1: Ratio of the FDTD and exact phase speeds ($\tilde{c}_p/c_p$) versus the discretization. Propagation in free space is assumed. Ideally the ratio would be unity for all discretizations. Courant numbers of $1/4$, $1/2$, and $3/4$ are considered.

Thus the phase speed in the FDTD grid is exactly what it is in the continuous world! This is true for all discretization.

Figure 7.1 shows a plot of the ratio of the FDTD and exact phase speeds as a function of discretization. Three different Courant numbers are used. Ideally the ratio would be unity for all discretizations. As can be seen, the greater the Courant number, the closer the curve is to ideal. A large Courant number is thus desirable for two reasons. First, the larger the Courant number, the greater the temporal step and hence the more quickly a simulation advances (i.e., each update represents a greater advance in time). Second, the larger the Courant number, the smaller the dispersion error. In one dimension a Courant number of unity is the greatest possible and, since there is no dispersion error with this Courant number, the corresponding time step is known as the magic time-step. Unfortunately a magic time-step does not exist in higher dimensions.

Figure 7.2 shows snapshots of Ricker wavelets propagating to the right that have been discretized at either 20 or 10 points per wavelength at the most energetic frequency (i.e., the parameter N_P discussed in Sec. 5.2.3 is either 20 or 10). The wavelets are propagating in grids that have a Courant number of either 1 or 0.5. In Figs. 7.2(a) and (b) the discretizations are 20 and 10, respectively, and the Courant number is unity. Since this corresponds to the magic time-step, the wavelets propagate without distortion. The discretizations in Figs. 7.2(c) and (d) are also 20 and 10, respectively, but now the Courant number is 0.5. The snapshots in (a) and (b) were taken after 100 time-steps while the snapshots in (c) and (d) were taken after 200 time-steps (since the time step is half as large in (c) and (d) as it is in (a) and (b), this ensures the snapshots are depicting the field at the same time). In Fig. 7.2(c) the distortion of the Ricker wavelet is visible in that the

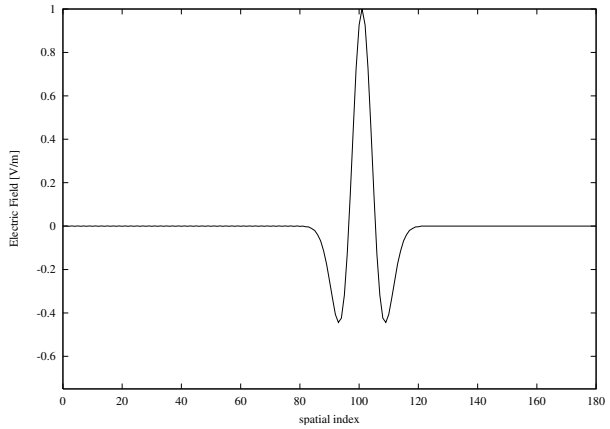

(a) $N_P = 20$, $S_c = 1$

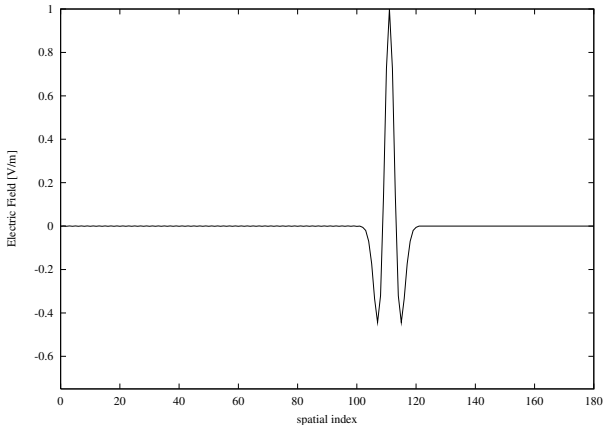

(b) $N_P = 10$, $S_c = 1$

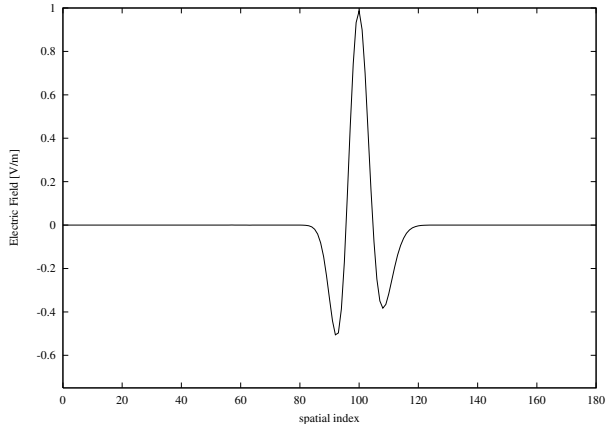

(c) $N_P = 20$, $S_c = 0.5$

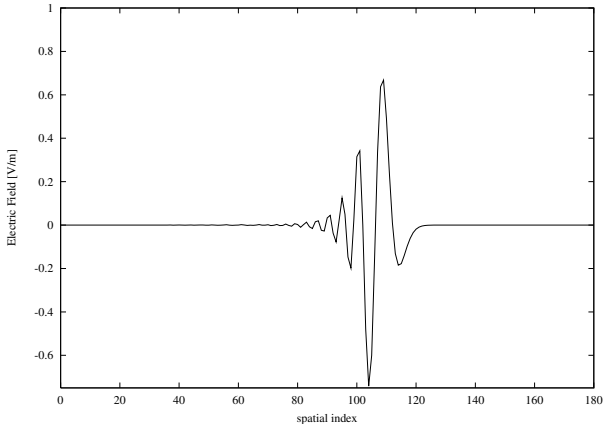

(d) $N_P = 10$, $S_c = 0.5$

Figure 7.2: Snapshots of Ricker wavelets with different discretization propagating in grids with different Courant numbers. (a) 20 points per wavelength at the most energetic frequency, i.e., $N_P = 20$, $S_c = 1$, (b) $N_P = 10$, $S_c = 1$, (c) $N_P = 20$, $S_c = 0.5$, and (d) $N_P = 10$, $S_c = 0.5$. The snapshots were taken after 100 time-steps for (a) and (b), and after 200 time-steps for (c) and (d).

function is no longer symmetric about the peak. In Fig. 7.2(d) the distortion caused by dispersion is rather extreme and the function is no longer recognizable as a Ricker wavelet. The reason that Fig. 7.2(d) is so much more distorted than Fig. 7.2(c) is that the spectral energy lies at a coarser discretization. The more coarsely a harmonic is discretized, the more dispersion it will suffer—the higher frequencies propagate more slowly than the lower frequencies. This causes the ringing that is evident on the trailing side of the pulse.

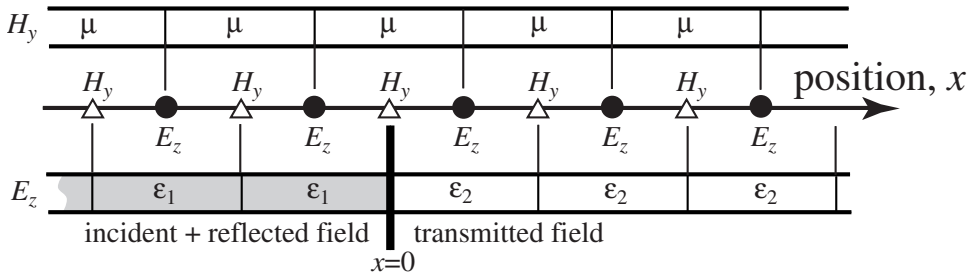

Figure 7.3: One-dimensional simulation where the permittivity changes abruptly at $x = 0$. The interface between the two media coincides with a magnetic-field node. The permeability is assumed to be constant throughout the computational domain. The figure depicts the nodes and the material values associated with their updates. The field to the left of the interface is the sum of the incident and reflected fields. The transmitted field exists to the right of the boundary.

7.5 Numeric Impedance

Let us return to (7.28) which nominally gave the numeric impedance and which is repeated below

$$\frac{\hat{E}_0}{\hat{H}_0} = -\frac{K_x}{\epsilon\Omega}. \tag{7.45}$$

The dispersion relation (7.35) expressed K_x in terms of Ω. Plugging this into (7.45) yields

$$\frac{\hat{E}_0}{\hat{H}_0} = -\frac{\sqrt{\mu\epsilon}\Omega}{\epsilon\Omega} = \sqrt{\frac{\mu}{\epsilon}} = \eta. \tag{7.46}$$

Thus, despite the inherent approximations in the FDTD method, the impedance in the grid is exactly the same as in the continuous world (this also holds in higher dimensions).

7.6 Analytic FDTD Reflection and Transmission Coefficients

Section 5.8.2 discussed the way in which an FDTD simulation could be used to measure the transmission coefficient associated with a planar interface. In this section, instead of using a simulation to measure the transmission coefficient, an expression will be derived that gives the transmission coefficient for the FDTD grid.

Consider a one-dimensional FDTD simulation as shown in Fig. 7.3. The permittivity changes abruptly at the magnetic field which is assumed to coincide with the interface at $x = 0$. The permeability is constant throughout the computational domain.

Assume there is an incident unit-amplitude plane wave propagating in the $+x$ direction. Because of the change in permittivity, a reflected field will exist to the left of the boundary which propagates in the $-x$ direction. Additionally, there will be a transmitted field which propagates to

the right of the boundary. The incident, reflected, and transmitted electrics fields are given by

$$\hat{E}_z^i[m,q] = \hat{E}_z^i[m]e^{j\omega q\Delta_t} = e^{-j\tilde{\beta}_1 m\Delta_x}e^{j\omega q\Delta_t}, \tag{7.47}$$

$$\hat{E}_z^r[m,q] = \hat{E}_z^r[m]e^{j\omega q\Delta_t} = \hat{\tilde{\Gamma}}e^{j\tilde{\beta}_1 m\Delta_x}e^{j\omega q\Delta_t}, \tag{7.48}$$

$$\hat{E}_z^t[m,q] = \hat{E}_z^t[m]e^{j\omega q\Delta_t} = \hat{\tilde{T}}e^{-j\tilde{\beta}_2 m\Delta_x}e^{j\omega q\Delta_t} \tag{7.49}$$

where $\hat{\tilde{\Gamma}}$ and $\hat{\tilde{T}}$ are the FDTD reflection and transmission coefficients, respectively. Note that all fields will have the common temporal phase factor $\exp(j\omega q\Delta_t)$. Therefore this term will not be explicitly written (its existence is implicit in the fact that we are doing harmonic analysis).

As shown in the previous section, the characteristic impedance in the FDTD grid is exact. Therefore the magnetic fields can be related to the electric fields in the same manner as they are in the continuous world, i.e.,

$$\hat{H}_y^i[m] = -\frac{1}{\eta_1}e^{-j\tilde{\beta}_1 m\Delta_x}, \tag{7.50}$$

$$\hat{H}_y^r[m] = \frac{\hat{\tilde{\Gamma}}}{\eta_1}e^{j\tilde{\beta}_1 m\Delta_x}, \tag{7.51}$$

$$\hat{H}_y^t[m] = -\frac{\hat{\tilde{T}}}{\eta_2}e^{-j\tilde{\beta}_2 m\Delta_x}. \tag{7.52}$$

The incident and reflected waves exist to the left of the interface and the transmitted field exists to the right of the interface. The magnetic field at the interface, i.e., the node at $x = 0$ is, in a sense, common to both the left and the right half-spaces. The field at this node can be described equally well as the sum of the incident and reflected waves or by the transmitted wave. This node enforces the continuity of the magnetic field across the boundary. Hence, just as in the continuous world, the fields are governed by the equation

$$-\frac{1}{\eta_1} + \frac{\hat{\tilde{\Gamma}}}{\eta_1} = -\frac{\hat{\tilde{T}}}{\eta_2}. \tag{7.53}$$

In the continuous world enforcing the continuity of the tangential electric and magnetic fields at a boundary yields two equations. These two equations can be used to solve for the reflection and transmission coefficients as was shown in Sec. 5.8.1. In FDTD, however, there are no electric field nodes that coincide with the interface (at least not with this geometry). Therefore continuity of the electric fields cannot be enforced directly nor is there a readily available second equation with which to solve for the reflection and transmission coefficients.

The necessary second equation is obtained by considering the update equation for the magnetic field at the interface. This node depends on the electric field to either side of the interface and hence ties the two half-spaces together. Specifically, the harmonic form of Faraday's law which governs the magnetic-field node at the interface can be used to write the following

$$\mu s_x^{1/2}\tilde{\partial}_t\hat{H}_y^q[m]\Big|_{x=0} = s_x^{1/2}\tilde{\partial}_x\hat{E}_z[m]\Big|_{x=0}, \tag{7.54}$$

$$\mu j\Omega\hat{H}_y[m]\Big|_{x=0} = \frac{1}{\Delta_x}\left(s_x^{1/2} - s_x^{-1/2}\right)\hat{E}_z^q[m]\Big|_{x=0}, \tag{7.55}$$

$$j\Omega\hat{H}_y[m]\Big|_{x=0} = \frac{1}{\mu\Delta_x}\left(\hat{\tilde{T}}e^{-j\tilde{\beta}_2\Delta_x/2} - \left[e^{j\tilde{\beta}_1\Delta_x/2} + \hat{\tilde{\Gamma}}e^{-j\tilde{\beta}_1\Delta_x/2}\right]\right). \tag{7.56}$$

In the last form of the equation, we have used the fact that the transmitted field is present when space is shifted a half spatial-step in the $+x$ direction relative to the boundary. Conversely the field is the sum of the incident and reflected waves when space is shifted a half spatial-step in the $-x$ direction relative to the boundary.

Equation (7.56) provides the second equation which, when coupled to (7.53), can be used to solve for the transmission and reflection coefficients. However, what is $\hat{H}_y[m]\Big|_{x=0}$? Since this node is on the interface, the expression for either the transmitted field or the sum of the incident and reflected field can be used. Using the transmitted field (evaluated at $m = 0$), the equation becomes

$$j\Omega\left(-\frac{\hat{\tilde{T}}}{\eta_2}\right) = \frac{1}{\mu\Delta_x}\left(\hat{\tilde{T}}e^{-j\tilde{\beta}_2\Delta_x/2} - \left[e^{j\tilde{\beta}_1\Delta_x/2} + \hat{\tilde{\Gamma}}e^{-j\tilde{\beta}_1\Delta_x/2}\right]\right). \tag{7.57}$$

Regrouping terms yields

$$e^{j\tilde{\beta}_1\Delta_x/2} + \hat{\tilde{\Gamma}}e^{-j\tilde{\beta}_1\Delta_x/2} = \left(e^{-j\tilde{\beta}_2\Delta_x/2} + j\frac{\Omega\mu\Delta_x}{\eta_2}\right)\hat{\tilde{T}}. \tag{7.58}$$

After multiplying through by $-\eta_1\exp(-j\tilde{\beta}_1\Delta_x/2)$, (7.53) becomes

$$e^{-j\tilde{\beta}_1\Delta_x/2} - \hat{\tilde{\Gamma}}e^{-j\tilde{\beta}_1\Delta_x/2} = \frac{\eta_1}{\eta_2}e^{-j\tilde{\beta}_1\Delta_x/2}\hat{\tilde{T}}. \tag{7.59}$$

Adding the left- and right-hand sides of (7.58) and (7.59) yields an expression that does not depend on the reflection coefficient. Multiplying this expression through by η_2 yields

$$\eta_2\left(e^{j\tilde{\beta}_1\Delta_x/2} + e^{-j\tilde{\beta}_1\Delta_x/2}\right) = \left(\eta_1 e^{-j\tilde{\beta}_1\Delta_x} + \eta_2 e^{-j\tilde{\beta}_2\Delta_x/2} + j\Omega\mu\Delta_x\right)\hat{\tilde{T}}. \tag{7.60}$$

Let us consider the third term in parentheses on the right-hand side. Recall from (7.35) that $\Omega = K_x/\sqrt{\mu\epsilon}$. Taking the material and propagation constants that pertain in the second medium,[†] we can write

$$\begin{aligned} j\Omega\mu\Delta_x &= j\frac{K_{x2}}{\sqrt{\mu\epsilon_2}}\mu\Delta_x, & (7.61)\\ &= j\sqrt{\frac{\mu}{\epsilon_2}}\frac{2}{\Delta_x}\sin\left(\frac{\tilde{\beta}_2\Delta_x}{2}\right)\Delta_x, & (7.62)\\ &= j\eta_2 2\left(\frac{e^{j\tilde{\beta}_2\Delta_x/2} - e^{-j\tilde{\beta}_2\Delta_x/2}}{j2}\right), & (7.63)\\ &= \eta_2\left(e^{j\tilde{\beta}_2\Delta_x/2} - e^{-j\tilde{\beta}_2\Delta_x/2}\right), & (7.64) \end{aligned}$$

where (7.22) was used to go from (7.61) to (7.62). Plugging this final form into (7.60), employing Euler's formula, and solving for the transmission coefficient yields

$$\hat{\tilde{T}} = \frac{2\eta_2\cos\left(\frac{\tilde{\beta}_1\Delta_x}{2}\right)}{\eta_1 e^{-j\tilde{\beta}_1\Delta_x/2} + \eta_2 e^{j\tilde{\beta}_2\Delta_x/2}}. \tag{7.65}$$

[†]As will be more obvious at the end of this derivation, we could instead select the material properties that pertain in the first medium and still obtain the same final result.

This can be compared to the exact transmission coefficient which is given in (5.88). At first it may appear that these are quite dissimilar. However, if the discretization is sufficiently small, the cosine and complex exponentials are close to unity (and become one as the discretization goes to zero). Hence the FDTD reflection coefficient reduces to the exact reflection coefficient as the discretization goes to zero.

The complex exponentials in (7.65) make it appear that the FDTD transmission coefficient is complex. This would impart a phase shift to the transmitted field that is not present in the continuous world. However, this is not the case—(7.65) can be simplified further. The one-dimensional dispersion relation (7.36) dictates that

$$\sin\left(\frac{\tilde{\beta}\Delta_x}{2}\right) = \frac{\sqrt{\epsilon\mu}\Delta_x}{\Delta_t}\sin\left(\frac{\omega\Delta_t}{2}\right). \tag{7.66}$$

Now consider the denominator of (7.65)

$$\begin{aligned}&\eta_1 e^{-j\tilde{\beta}_1\Delta_x/2} + \eta_2 e^{j\tilde{\beta}_2\Delta_x/2} \\ &= \eta_1\left(\cos\left(\frac{\tilde{\beta}_1\Delta_x}{2}\right) - j\sin\left(\frac{\tilde{\beta}_1\Delta_x}{2}\right)\right) + \eta_2\left(\cos\left(\frac{\tilde{\beta}_2\Delta_x}{2}\right) + j\sin\left(\frac{\tilde{\beta}_2\Delta_x}{2}\right)\right)\end{aligned} \tag{7.67}$$

Using (7.66) to convert the sine terms and employing the definition of impedance, the denominator can be written

$$\begin{aligned}&\eta_1\cos\left(\frac{\tilde{\beta}_1\Delta_x}{2}\right) + \eta_2\cos\left(\frac{\tilde{\beta}_2\Delta_x}{2}\right) \\ &\quad -j\sqrt{\frac{\mu}{\epsilon_1}}\frac{\sqrt{\epsilon_1\mu}\Delta_x}{\Delta_t}\sin\left(\frac{\omega\Delta_t}{2}\right) + j\sqrt{\frac{\mu}{\epsilon_2}}\frac{\sqrt{\epsilon_2\mu}\Delta_x}{\Delta_t}\sin\left(\frac{\omega\Delta_t}{2}\right).\end{aligned} \tag{7.68}$$

Upon canceling the ϵ's, the imaginary parts cancel and hence the denominator is purely real. Therefore another expression for the FDTD transmission coefficient is

$$\hat{\tilde{T}} = \frac{2\eta_2\cos\left(\frac{\tilde{\beta}_1\Delta_x}{2}\right)}{\eta_2\cos\left(\frac{\tilde{\beta}_2\Delta_x}{2}\right) + \eta_1\cos\left(\frac{\tilde{\beta}_1\Delta_x}{2}\right)}. \tag{7.69}$$

Combining this with (7.53) yields the reflection coefficient

$$\hat{\tilde{\Gamma}} = \frac{\eta_2\cos\left(\frac{\tilde{\beta}_2\Delta_x}{2}\right) - \eta_1\cos\left(\frac{\tilde{\beta}_1\Delta_x}{2}\right)}{\eta_2\cos\left(\frac{\tilde{\beta}_2\Delta_x}{2}\right) + \eta_1\cos\left(\frac{\tilde{\beta}_1\Delta_x}{2}\right)}. \tag{7.70}$$

Because the permeability is assumed to be constant throughout the computational domain, the reflection and transmission coefficients can be written as

$$\hat{\tilde{T}} = \frac{2\sqrt{\epsilon_1}\cos\left(\frac{\tilde{\beta}_1\Delta_x}{2}\right)}{\sqrt{\epsilon_1}\cos\left(\frac{\tilde{\beta}_2\Delta_x}{2}\right) + \sqrt{\epsilon_2}\cos\left(\frac{\tilde{\beta}_1\Delta_x}{2}\right)}, \tag{7.71}$$

$$\hat{\tilde{\Gamma}} = \frac{\sqrt{\epsilon_1}\cos\left(\frac{\tilde{\beta}_2\Delta_x}{2}\right) - \sqrt{\epsilon_2}\cos\left(\frac{\tilde{\beta}_1\Delta_x}{2}\right)}{\sqrt{\epsilon_1}\cos\left(\frac{\tilde{\beta}_2\Delta_x}{2}\right) + \sqrt{\epsilon_2}\cos\left(\frac{\tilde{\beta}_1\Delta_x}{2}\right)}. \tag{7.72}$$

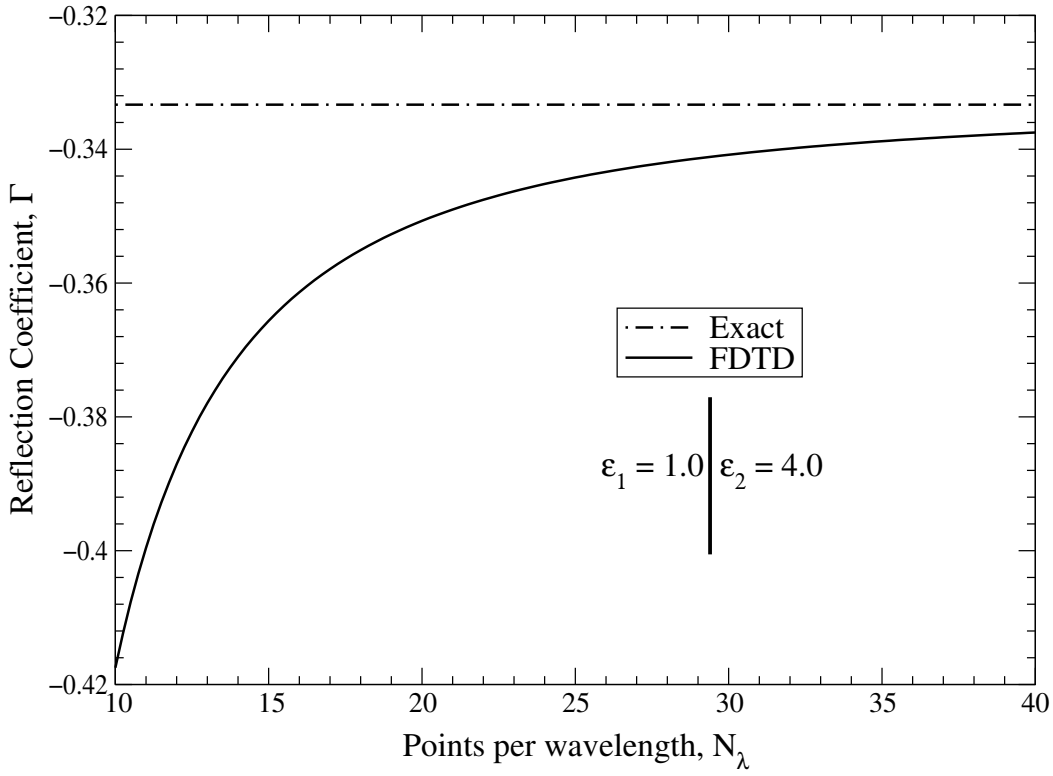

Figure 7.4: Reflection coefficient versus discretization for a wave traveling from free space to a dielectric with a relative permittivity of 4.0 (i.e., $\epsilon_{r1} = 1.0$ and $\epsilon_{r2} = 4.0$). The discretization N_λ shown on the horizontal axis is that which pertains to free space. (These values should be halved to give the discretization pertaining to the dielectric.)

Figure 7.4 shows a plot of the FDTD reflection coefficient versus the points per wavelength (in free space) when a wave is incident from free space to a dielectric with a relative permittivity of 4.0. For these materials the exact reflection coefficient, which is independent of the discretization and is also shown in the plot, is $\hat{\Gamma} = (1-2)/(1+2) = -1/3$. When the discretization is 10 points per wavelength the FDTD reflection coefficient is nearly -0.42 which corresponds to an error of approximately 26 percent. This error is rather large, but one must keep in mind that in the dielectric the discretization is only five points per wavelength. This coarse discretization affects the quality of the results throughout the computational domain, not just in the dielectric. Thus, even though one may ultimately be interested in the fields over only a portion of the computational domain, nevertheless, one must assure that a proper level of discretization is maintained throughout the grid.

7.7 Reflection from a PEC

A perfect electric conductor is realized by setting to zero electric field nodes. Let us assume that one wants to continue to define the interface as shown in Fig. 7.3, i.e., the boundary is assumed to coincide with a magnetic-field node. The new scenario is shown in Fig. 7.5. The electric-field

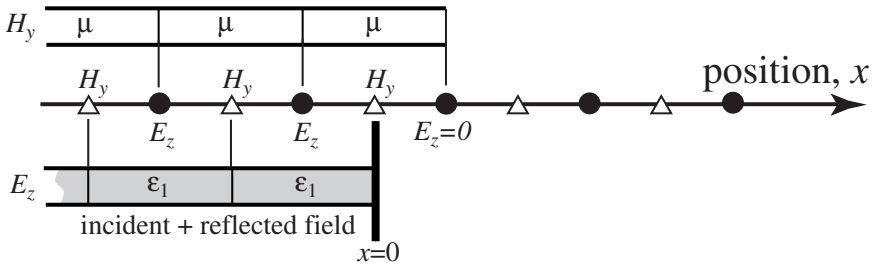

Figure 7.5: One-dimensional space with a perfect electric conductor realized by setting an electric field node to zero. No fields propagate beyond the zeroed node. The reference point $x = 0$ is still assumed to coincide with a magnetic-field node.

node to the right of the interface is set to zero. We now seek to find the reflection coefficient for this case. There is no transmitted field so the transmission coefficient $\hat{\tilde{T}}$ must be zero. That might lead one to think, given (7.53), that the reflection coefficient must be -1 as it is in the continuous world for a PEC boundary. However, that is not correct. Implicit in (7.53) is the assumption that the magnetic field is continuous across the interface. When a PEC is present, this is no longer the case. In the continuous world the discontinuity in the magnetic field is accounted for by a surface current.

When a PEC is present there is only one unknown, the reflection coefficient can be obtained from a single equation since the transmission coefficient is known *a priori*. This equation is provided, as before, by the update equation of the magnetic-field node at the interface. To this end, (7.56) is used with the transmission coefficient set to zero. Also, instead of using the transmitted form of the magnetic field at the interface as was done to obtain (7.57), the sum of the incident and reflected fields is used to obtain:

$$j\Omega\left(-\frac{1}{\eta_1}+\frac{\hat{\tilde{\Gamma}}}{\eta_1}\right)=\frac{1}{\mu\Delta_x}\left(0-\left[e^{j\tilde{\beta}_1\Delta_x/2}+\hat{\tilde{\Gamma}}e^{-j\tilde{\beta}_1\Delta_x/2}\right]\right). \tag{7.73}$$

Solving for the reflection coefficient yields

$$\hat{\tilde{\Gamma}}_{\text{PEC}}=\frac{j\Omega\mu\Delta_x-\eta_1 e^{j\tilde{\beta}_1\Delta_x/2}}{j\Omega\mu\Delta_x+\eta_1 e^{-j\tilde{\beta}_1\Delta_x/2}}. \tag{7.74}$$

As was shown in (7.61)–(7.64), the factor $j\Omega\mu\Delta_x$ can be expressed in terms of the impedance and a difference of complex exponentials. Employing such a conversion allows the reflection coefficient to be written as

$$\hat{\tilde{\Gamma}}_{\text{PEC}}=-e^{-j\tilde{\beta}_1\Delta_x}. \tag{7.75}$$

Note that the magnitude of the reflection coefficient is unity so that the entire incident field, regardless of the frequency, is reflected from the interface.

It appears that the FDTD reflection coefficient for a PEC is introducing a shift that is not present in the continuous world. However, this is being a bit unfair to the FDTD method. The location of the PEC boundary really corresponds to the electric-field node that was set to zero. Thus, one should really think of the PEC boundary existing at $x = \Delta_x/2$.

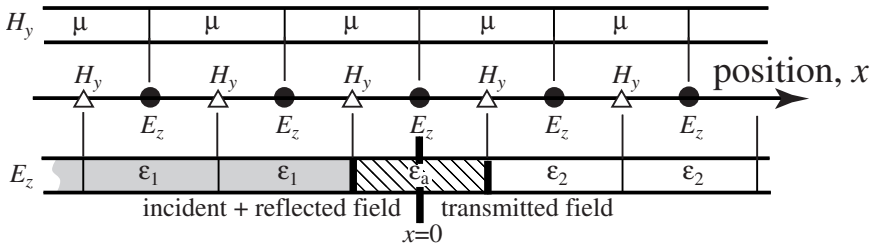

Figure 7.6: One-dimensional space with a discontinuity in permittivity. The interface in the continuous world corresponds to an electric-field node in the FDTD grid. The permittivity to the left of the interface is ϵ_1 and is ϵ_2 to the right. These values are dictated by those in the continuous world. The permittivity of the node at the interface is ϵ_a.

In the continuous world, let us consider a scenario where the origin is located a distance $\Delta_x/2$ in front of a PEC boundary. In that case the incident and reflected fields must sum to zero at $x = \Delta_x/2$, i.e.,

$$E^{\text{inc}}(x) + E^{\text{ref}}(x)\big|_{x=\Delta_x/2} = 0, \tag{7.76}$$

$$e^{-j\beta_1\Delta_x/2} + \hat{\Gamma}e^{j\beta_1\Delta_x/2} = 0. \tag{7.77}$$

Thus, in the continuous world the reflection coefficient is

$$\hat{\Gamma} = -e^{-j\beta_1\Delta_x}. \tag{7.78}$$

When first comparing (7.75) and (7.78) it may appear that in this case the FDTD reflection coefficient is exact. However the two differ owing to the fact that phase constants β_1 and $\tilde{\beta}_1$ are different in the two domains.

7.8 Interface Aligned with an Electric-Field Node

There are situations which necessitate that a discontinuity in permittivity be modeled as coinciding with an electric field node. The permittivity that should be used to either side of the interface is unambiguous but the permittivity of the node at the interface is open to question since it is neither in one half-space nor the other. This scenario was mentioned in Sec. 3.11 where it was suggested that the average permittivity be used for the node at the interface. In this section we wish to provide a more rigorous analysis to justify this permittivity. For now, let the permittivity of the node at the interface be ϵ_a as depicted in Fig. 7.6. The goal now is to find the reflection or transmission coefficients for this geometry and find the value of ϵ_a which yields the best agreement with the continuous-world values.

Although the origin $x = 0$ has shifted from that which was assumed in the previous section, the incident, reflected, and transmitted fields are still assumed to be given by (7.47)–(7.49) and (7.50)–(7.52). The electric-field node at the interface is a member of both half-spaces, i.e., the field is the same whether considered to be the sum of the incident and reflected field or simply to be the transmitted field. This yields a boundary condition of

$$1 + \hat{\tilde{\Gamma}} = \hat{\tilde{T}}. \tag{7.79}$$

Another equation relating the transmission and reflection coefficients is obtained via the update equation for the electric-field node at the interface. Ampere's law evaluated at the interface is

$$j\epsilon_a\Omega\hat{\tilde{T}} = \frac{1}{\Delta_x}\left(-\frac{\hat{\tilde{T}}}{\eta_2}e^{-j\tilde{\beta}_2\Delta_x/2} - \left[-\frac{1}{\eta_1}e^{j\tilde{\beta}_1\Delta_x/2} + \frac{\hat{\tilde{\Gamma}}}{\eta_1}e^{-j\tilde{\beta}_1\Delta_x/2}\right]\right). \tag{7.80}$$

Using (7.79) $\hat{\tilde{T}}$ can be replaced with $1+\hat{\tilde{\Gamma}}$. Then solving for $\hat{\tilde{\Gamma}}$ yields

$$\hat{\tilde{\Gamma}} = \frac{\eta_2 e^{j\tilde{\beta}_1\Delta_x/2} - \eta_1 e^{-j\tilde{\beta}_2\Delta_x/2} - j\eta_1\eta_2\epsilon_a\Omega\Delta_x}{\eta_2 e^{-j\tilde{\beta}_1\Delta_x/2} + \eta_1 e^{-j\tilde{\beta}_2\Delta_x/2} + j\eta_1\eta_2\epsilon_a\Omega\Delta_x}. \tag{7.81}$$

The term $\Omega\Delta_x$ can be written as

$$\begin{aligned}
\Omega\Delta_x &= \frac{2}{\Delta_t}\sin\left(\frac{\omega\Delta_t}{2}\right)\Delta_x, &(7.82)\\
&= 2c\frac{\Delta_x}{c\Delta_t}\sin\left(\frac{\omega\Delta_t}{2}\right), &(7.83)\\
&= 2c\frac{1}{S_c}\sin\left(\frac{2\pi c}{N_\lambda\Delta_x}\frac{\Delta_t}{2}\right), &(7.84)\\
&= 2c\frac{1}{S_c}\sin\left(\frac{\pi}{N_\lambda}S_c\right). &(7.85)
\end{aligned}$$

The conversion of $\omega\Delta_t/2$ to $\pi S_c/N_\lambda$ was discussed in connection with (5.74). Using this last form of $\Omega\Delta_x$, the third term in the numerator and denominator of (7.81) can be written

$$\begin{aligned}
j\eta_1\eta_2\epsilon_a\Omega\Delta_x &= j\sqrt{\frac{\mu}{\epsilon_0\epsilon_{r1}}}\sqrt{\frac{\mu}{\epsilon_0\epsilon_{r2}}}2c\epsilon_0\epsilon_{ra}\frac{1}{S_c}\sin\left(\frac{\pi}{N_\lambda}S_c\right), &(7.86)\\
&= j\frac{\epsilon_{ra}}{\sqrt{\epsilon_{r1}\epsilon_{r2}}}\frac{\mu}{\epsilon_0}2c\epsilon_0\frac{1}{S_c}\sin\left(\frac{\pi}{N_\lambda}S_c\right), &(7.87)\\
&= j\frac{\epsilon_{ra}}{\sqrt{\epsilon_{r1}\epsilon_{r2}}}2\mu c\frac{1}{S_c}\sin\left(\frac{\pi}{N_\lambda}S_c\right), &(7.88)
\end{aligned}$$

where ϵ_{ra} is the relative permittivity of the node at the interface.

Assume that the permeability throughout the computational domain is the permeability of free space so that μc in (7.88) can be written $\mu_0 c = \mu_0/\sqrt{\mu_0\epsilon_0} = \sqrt{\mu_0/\epsilon_0} = \eta_0$. The reflection coefficient (7.81) can now be written as

$$\hat{\tilde{\Gamma}} = \frac{\frac{1}{\sqrt{\epsilon_{r2}}}\eta_0 e^{j\tilde{\beta}_1\Delta_x/2} - \frac{1}{\sqrt{\epsilon_{r1}}}\eta_0 e^{-j\tilde{\beta}_2\Delta_x/2} - j\frac{\epsilon_{ra}}{\sqrt{\epsilon_{r1}\epsilon_{r2}}}\eta_0\frac{2}{S_c}\sin\left(\frac{\pi}{N_\lambda}S_c\right)}{\frac{1}{\sqrt{\epsilon_{r2}}}\eta_0 e^{-j\tilde{\beta}_1\Delta_x/2} + \frac{1}{\sqrt{\epsilon_{r1}}}\eta_0 e^{-j\tilde{\beta}_2\Delta_x/2} + j\frac{\epsilon_{ra}}{\sqrt{\epsilon_{r1}\epsilon_{r2}}}\eta_0\frac{2}{S_c}\sin\left(\frac{\pi}{N_\lambda}S_c\right)}. \tag{7.89}$$

Multiplying numerator and denominator by $\sqrt{\epsilon_{r1}\epsilon_{r2}}/\eta_0$ yields

$$\hat{\tilde{\Gamma}} = \frac{\sqrt{\epsilon_{r1}}e^{j\tilde{\beta}_1\Delta_x/2} - \sqrt{\epsilon_{r2}}e^{-j\tilde{\beta}_2\Delta_x/2} - j\epsilon_{ra}\frac{2}{S_c}\sin\left(\frac{\pi}{N_\lambda}S_c\right)}{\sqrt{\epsilon_{r1}}e^{-j\tilde{\beta}_1\Delta_x/2} + \sqrt{\epsilon_{r2}}e^{-j\tilde{\beta}_2\Delta_x/2} + j\epsilon_{ra}\frac{2}{S_c}\sin\left(\frac{\pi}{N_\lambda}S_c\right)}. \tag{7.90}$$

As is often the case, the expression for a quantity in the FDTD grid bears little resemblance to that in the continuous world. However, as the discretization goes to zero (i.e., N_λ goes to infinity), (7.90) does indeed reduce to the reflection coefficient in the continuous world.

The first two terms in the numerator and denominator of (7.90) depend on the material constants to either side of the interface while the third term depends on the permittivity at the interface, the Courant number, and the number of points per wavelength (in continuous-world free space). We now seek the value of ϵ_a (or the corresponding relative permittivity ϵ_{ra}) which minimizes the difference between the reflection coefficient in the continuous world and the one in the FDTD world. It is important to note that in general the FDTD reflection coefficient in this case is truly complex—there will be a phase shift imparted that does not exist in the continuous world.

Before going further with the analysis, let us consider an example with specific parameters and graphically solve for the optimum value of ϵ_a. Let $\epsilon_{r1} = 1$, $\epsilon_{r2} = 4$, and the discretization be 10 points per wavelength. In this case the reflection coefficient in the continuous world is $-1/3$ (independent of frequency). Figure 7.7 shows the FDTD reflection coefficient in the complex plane for various values of ϵ_{ra}. The continuous-world result, i.e., the exact result, is a single point on the negative real axis. As ϵ_{ra} varies a curve is obtained in the complex plane which is closest to the exact value when ϵ_{ra} is 2.5 which is the arithmetic average of 1 and 4. Thus the optimum value for the interface permittivity is the average of the permittivities to either side. However, these results are only for a specific discretization and for one set of permittivities. Is the average value the optimum one for all permittivities and discretizations?

To answer this question, let us return to (7.81) and separate the numerator and denominator into real and imaginary parts. The result is

$$\hat{\tilde{\Gamma}} = \frac{\eta_2 \cos(\kappa_1) - \eta_1 \cos(\kappa_2) + j\left[\eta_2 \sin(\kappa_1) + \eta_1 \sin(\kappa_2) - \eta_1\eta_2\epsilon_a\Omega\Delta_x\right]}{\eta_2 \cos(\kappa_1) + \eta_1 \cos(\kappa_2) - j\left[\eta_2 \sin(\kappa_1) + \eta_1 \sin(\kappa_2) - \eta_1\eta_2\epsilon_a\Omega\Delta_x\right]} \tag{7.91}$$

where

$$\kappa_1 = \tilde{\beta}_1\Delta_x/2, \tag{7.92}$$

$$\kappa_2 = \tilde{\beta}_2\Delta_x/2. \tag{7.93}$$

The continuous-world reflection coefficient is purely real and thus any imaginary part is an error. Furthermore, the imaginary part goes to zero as the discretization goes to zero. Let us consider just this imaginary part of the numerator and denominator. The $\sin(\kappa)$ terms can be related to the K terms which have been used previously—one merely had to multiply (and divide) by $2/\Delta_x$. Thus the imaginary part can be written

$$\eta_2\frac{2}{\Delta_x}\sin(\kappa_1)\frac{\Delta_x}{2} + \eta_1\frac{2}{\Delta_x}\sin(\kappa_2)\frac{\Delta_x}{2} - \eta_1\eta_2\epsilon_a\Omega\Delta_x = \eta_1\eta_2\frac{\Delta_x}{2}\left(\frac{1}{\eta_1}K_1 + \frac{1}{\eta_2}K_2 - 2\epsilon_a\Omega\right). \tag{7.94}$$

From the dispersion relation 7.33 we know that $K_1 = \sqrt{\mu\epsilon_1}\Omega$ and $K_2 = \sqrt{\mu\epsilon_2}\Omega$. This allows the imaginary part of the numerator and denominator of the reflection coefficient to be written

$$\eta_1\eta_2\frac{\Delta_x}{2}\Omega\left(\epsilon_1 + \epsilon_2 - 2\epsilon_a\right). \tag{7.95}$$

Setting ϵ_a equal to $(\epsilon_1 + \epsilon_2)/2$ will yield zero for this imaginary term. Hence the average permittivity is the optimum value for all permittivities and discretizations! Using the average permittivity

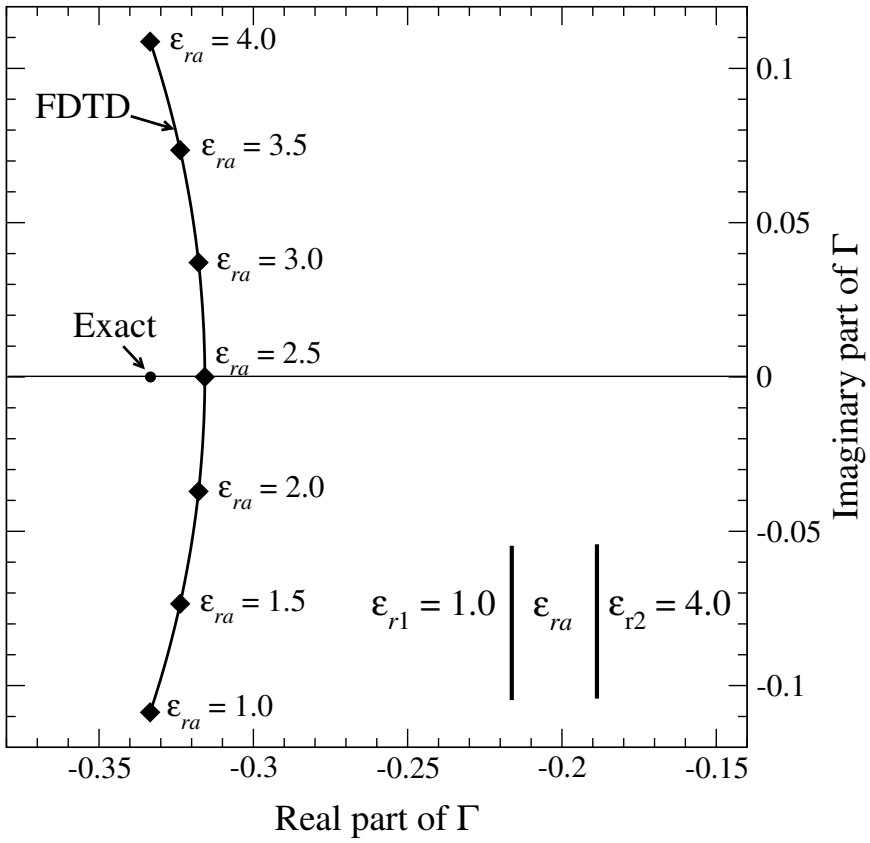

Figure 7.7: Curve showing the FDTD reflection coefficient in the complex plane as a function of ϵ_{ra} as ϵ_{ra} varies between the relative permittivity to the left of the interface ($\epsilon_{ra} = 1$) and the relative permittivity to the right of the interface ($\epsilon_{ra} = 4$). The value of ϵ_{ra} which minimizes the difference between the FDTD reflection coefficient and the exact value of $-1/3$ is the average permittivity, i.e., $\epsilon_{ra} = 2.5$.

yields reflection and transmission coefficients of

$$\hat{\tilde{\Gamma}} = \frac{\eta_2 \cos(\kappa_1) - \eta_1 \cos(\kappa_2)}{\eta_2 \cos(\kappa_1) + \eta_1 \cos(\kappa_2)}, \tag{7.96}$$

$$\hat{\tilde{T}} = \frac{2\eta_2 \cos(\kappa_1)}{\eta_2 \cos(\kappa_1) + \eta_1 \cos(\kappa_2)}. \tag{7.97}$$

Note that these equations appear almost identical to those which pertained to the case of an abrupt interface (i.e., when no averaging is done and the resulting reflection and transmission coefficients are (7.70) and (7.69)). However, these equations differ in the arguments of the cosine terms and, in fact, it can be shown that the abrupt boundary is slightly more accurate than the one which is implemented with the average permittivity at the interface. Nevertheless, when the situation calls for the interface to coincide with a tangential electric field, the average permittivity is the optimum one to use.